


Article

Using 1D Thermal Modeling to Evaluate Formation Models of Mafic-Ultramafic Intrusions and Associated Sulfide Cu-Ni-PGE Mineralization

Dmitry Stepenshchikov and Nikolay Groshev * 

Geological Institute, Kola Science Centre, Russian Academy of Sciences, Apatity 184209, Russia

* Correspondence: n.groshev@ksc.ru

Abstract: In this paper, we trace the thermal history of the mafic–ultramafic intrusions of the Monchegorsk (MC), Fedorova–Pana (FPC), and Norilsk ore-bearing complexes (NC) using an upgraded version of the author’s software Gehenna 2.2. It is shown that a key role in the concentration of sulfides in the lower parts of the intrusions belongs to the preliminary heating of the host rocks by early magmatic influxes. In the presence of late ore-bearing magmatic phases of a relatively small volume, the pattern of sulfide distribution within such a phase can be used to estimate the time gap with the main influx. Thermal modeling shows that the Gabbro-10 massif, an additional ore-bearing phase of the Nyud-Poaz intrusion of the MC, is separated from the main influx by a time gap of no more than 100 ka, while the minimum gap between the magmatic phases of the Fedorova intrusion of the FPC is 650–700 ka. The development of a hornfels halo around mafic–ultramafic rocks makes it possible to estimate the duration of the process of continuous magma flow inside intrusions, which, as an example from the Kharaelakh intrusion of the NC shows, can reach 1000 years and more. Thermal modeling is recommended both for formulating genetic hypotheses and for testing different scenarios for the formation of sulfide Cu-Ni-PGE mineralization in mafic–ultramafic complexes.

Keywords: thermal modeling; mafic–ultramafic; layered intrusion; sulfide; contact-style Cu-Ni-PGE mineralization; Kola region; Norilsk ore-bearing intrusions



Citation: Stepenshchikov, D.; Groshev, N. Using 1D Thermal Modeling to Evaluate Formation Models of Mafic-Ultramafic Intrusions and Associated Sulfide Cu-Ni-PGE Mineralization. *Minerals* **2023**, *13*, 1046. <https://doi.org/10.3390/min13081046>

Academic Editors: Evgeniy Kislov and Shoji Arai

Received: 11 June 2023

Revised: 12 July 2023

Accepted: 19 July 2023

Published: 6 August 2023



Copyright: © 2023 by the authors. Licensee MDPI, Basel, Switzerland. This article is an open access article distributed under the terms and conditions of the Creative Commons Attribution (CC BY) license (<https://creativecommons.org/licenses/by/4.0/>).

1. Introduction

Mafic–ultramafic intrusive complexes [1–3], solidified in the Earth’s crust at a depth of several kilometers, are an important source of critical metals, such as copper, nickel, cobalt, and platinum-group elements (PGEs). Prominent deposits of these metals are being actively mined in the Bushveld layered complex in South Africa [4]. Despite a long history of study, large new orebodies in the Bushveld continue to be discovered, as exemplified by the Flatreef deposit [5]. In many regions of the world, exploration activities within mafic–ultramafic complexes are aimed at discovering such orebodies [6,7]. Particular success in recent decades has been achieved within the Fennoscandian Shield [8], where several large deposits with total platinum metal resources of several thousand tons were discovered (e.g., Suhanko, Fedorova Tundra).

Genetic models of an individual deposit are formed throughout the whole history of its investigation and determine the prospecting strategy. In the conditions of a limited amount of factual material at the initial stages, the development of genetic models is facilitated by various methods of mathematical modeling, which allow for formulating the first working hypotheses without significant investments into their further empirical testing.

In this article, we discuss a series of examples of using 1D thermal modeling to identify critical geological processes that are of key importance to the formation of PGE-bearing sulfide mineralization in mafic–ultramafic complexes. Understanding the thermal history is of great importance for igneous mafic–ultramafic complexes, since an estimation of maximum temperature gives insight into the magma fertility for base and noble metals, and

timespans of keeping this temperature may give insight into the potential of the intrusions to develop sulfide Cu-Ni-PGE mineralization. In addition, thermal modeling allows us to reconstruct contact rock haloes and to provide information about the multiply replenished nature of the igneous system, which may indicate high potential for mineralization. The main examples are sulfide deposits in the Monchegorsk and Fedorova–Pana complexes within the Kola region, as well as ore-bearing intrusions in the Norilsk region.

2. Research Methodology and Description of the Gehenna Program

Mafic–ultramafic complexes are formed in the earth’s crust from high-temperature magma (1200–1300 °C) [1]. Many problems of their formation are debatable, including problems of space [9], the problem of duration [10,11], and others. In our study, we intentionally simplify the model and take into account only the heat transfer from hot magma to host rocks in a one-dimensional format.

2.1. Thermal Diffusivity Equation

Heat transfer in the rock mass is described using the one-dimensional heat conduction equation

$$\frac{\partial T}{\partial t} = k \frac{\partial^2 T}{\partial x^2} \quad (1)$$

where $T = T(x,t)$ —temperature, x —distance from the surface, t —time, k —thermal diffusivity. The initial conditions $T(x,0) = \varphi(x)$ set the initial heating of the stratum, and $T(0,t) = t_0$ and $T(x_{\max},t) = t_{\max}$ are the temperatures at its extreme points (it is assumed that the temperature on the surface and at depth dissipates). The value of thermal diffusivity varies within certain limits depending on the type of substance; here, we take it as homogeneous in space and equal to $2 \times 10^{-6} \text{ m}^2\text{s}^{-1}$ [12].

A discrete solution of this equation, provided as supplementary in [13], allows us to estimate the temperature at some arbitrary point in the stratum that has been heated from a hot source:

$$T_i^{n+1} = T_i^n + k\Delta t \left(\frac{T_{i+1}^n - 2T_i^n + T_{i-1}^n}{(\Delta x)^2} \right) \quad (2)$$

The advantage of a discrete solution is the possibility of adjusting the temperature conditions at different times in different parts of the sequence, which can be interpreted as magma intrusion. Varying such adjustments allows for modeling different scenarios of intrusive processes.

2.2. Gehenna Program

The FPC-based Gehenna 2.2 program is intended for modeling thermal processes associated with the extended-in-time formation of intrusive bodies. Similar to the first version of the software [14], a list of initial data is specified: each entry indicates a moment of emplacement of a separate intrusive body, its thickness, depth of occurrence (along the roof), temperature, and duration of saving the initial temperature. The result in the new software version is displayed in the form of a “thermogram” in the coordinates of depth and time, for which the range of displayed depths and time are pre-set. Temperature, depth, and time are displayed for each point in the resulting chart. The program interface with a demo test example is shown in Figure 1.

The calculations are based on the solution of the one-dimensional heat equation via the finite difference method. Calculation accuracy depends on the predetermined thickness of an elementary layer. Additionally, a number of temperature parameters of the host environment are introduced (thermal diffusivity, geothermal gradient, and surface temperature).

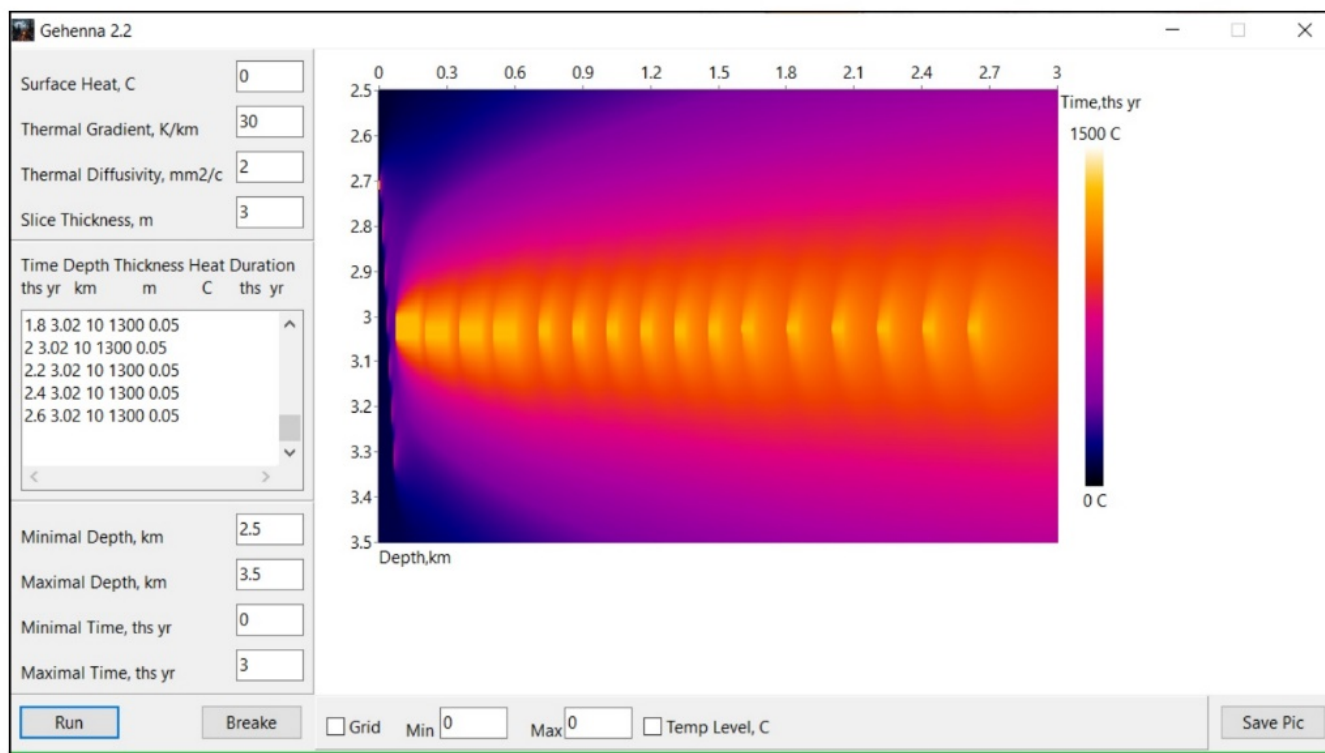


Figure 1. Gehenna 2.2 interface.

The program and input parameters for the used models are available in the Supplementary File.

3. Results

The main sources of PGE in layered mafic–ultramafic intrusions are laterally extended reefs associated with internal stratigraphy of intrusions. The Merensky, Platreef, UG-2, and J-M reef deposits are well known, developed, and supply the majority of the global PGE market [15]. In recent years, the importance of another PGE mineralization, located at the base of intrusions and attributed to contact style, has sharply increased. Firstly, this is due to the discovery of deep Platreef horizons in the Bushveld, namely the abovementioned Flatreef deposit [5]. Secondly, considering Fennoscandian layered intrusions (Figure 2), contact-style PGE mineralization has greater prospects here in view of the ratio of volumes of discovered recourses compared with the mineralization from internal stratigraphy. Currently, Suhanko (Finland) and Fedorova Tundra (Russia) are the two main projects in the region, targeting contact-style mineralization and close to the mining stage [16,17].

Prospecting and thematic works from recent years have revealed a great potential for contact-style PGE mineralization within the Paleoproterozoic Monchegorsk Complex, located about 120 km south of Murmansk, as well as within the Fedorova–Pana Complex, about 100 km southeast of the Monchegorsk (Figure 2). The main results of this study are thermal models for the formation of PGE mineralization presented by disseminated sulfide at the base of intrusions.

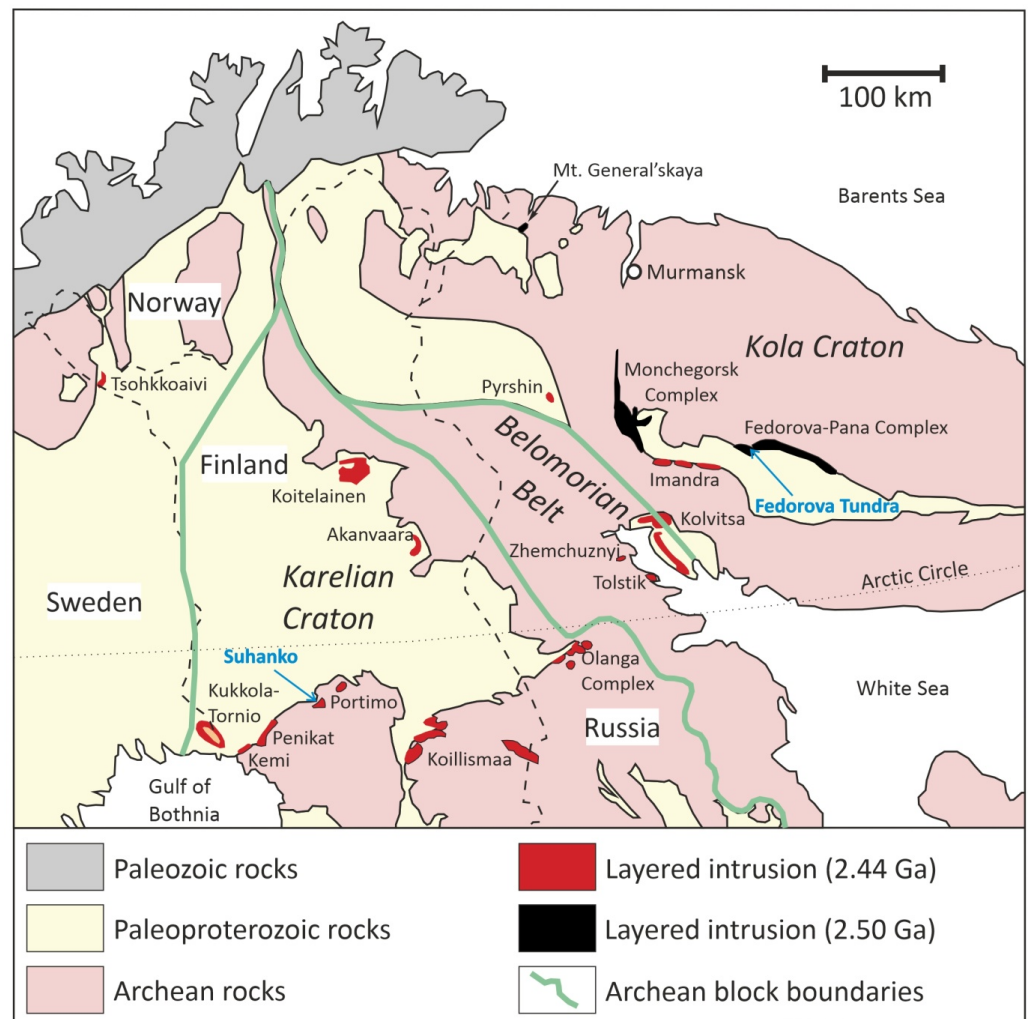


Figure 2. Simplified geologic map of the northeastern part of the Fennoscandian Shield, showing the position of Paleoproterozoic layered mafic–ultramafic intrusions. Modified from [18].

3.1. Monchegorsk Complex

The Monchegorsk Complex includes two spatially separate intrusions with a total area of about 550 km², the predominantly ultramafic Monchepluton (~65 km²) and the mafic Main Ridge (~485 km²), which are separated by a large fault trending northwest (Figure 3, inset). Monchepluton has a crescent-like shape and consists of six mountains representing two subchambers: the first ultramafic subchamber is represented by massifs of Mts. Nittis, Kumuzhya, Travyanaya (NKT) and Sopcha, the second ultramafic–mafic subchamber includes massifs of Mts. Nyud and Poaz. The complex of the Main Ridge includes the Volchetundra, Monchetundra, and Chunatundra intrusions, which are three tectonic blocks of an originally single intrusion with a thickness of more than 2500 m [19]. All intrusions of the Monchegorsk Complex contain sulfide mineralization enriched to varying degrees with PGE, Cu, and Ni. However, a significant part of Main Ridge located on the territory of the Lapland Biosphere Reserve is closed for economic activity. Based on the ore diversity of the complex, hosting chromite layers [20], sulfide dissemination near the contact and within layered cumulates [13], PGE reefs [21], the magnetite layer [22], as well as vertical veins of massive sulfides [23], the Monchepluton can be considered as a type section of ore-bearing layered intrusions.

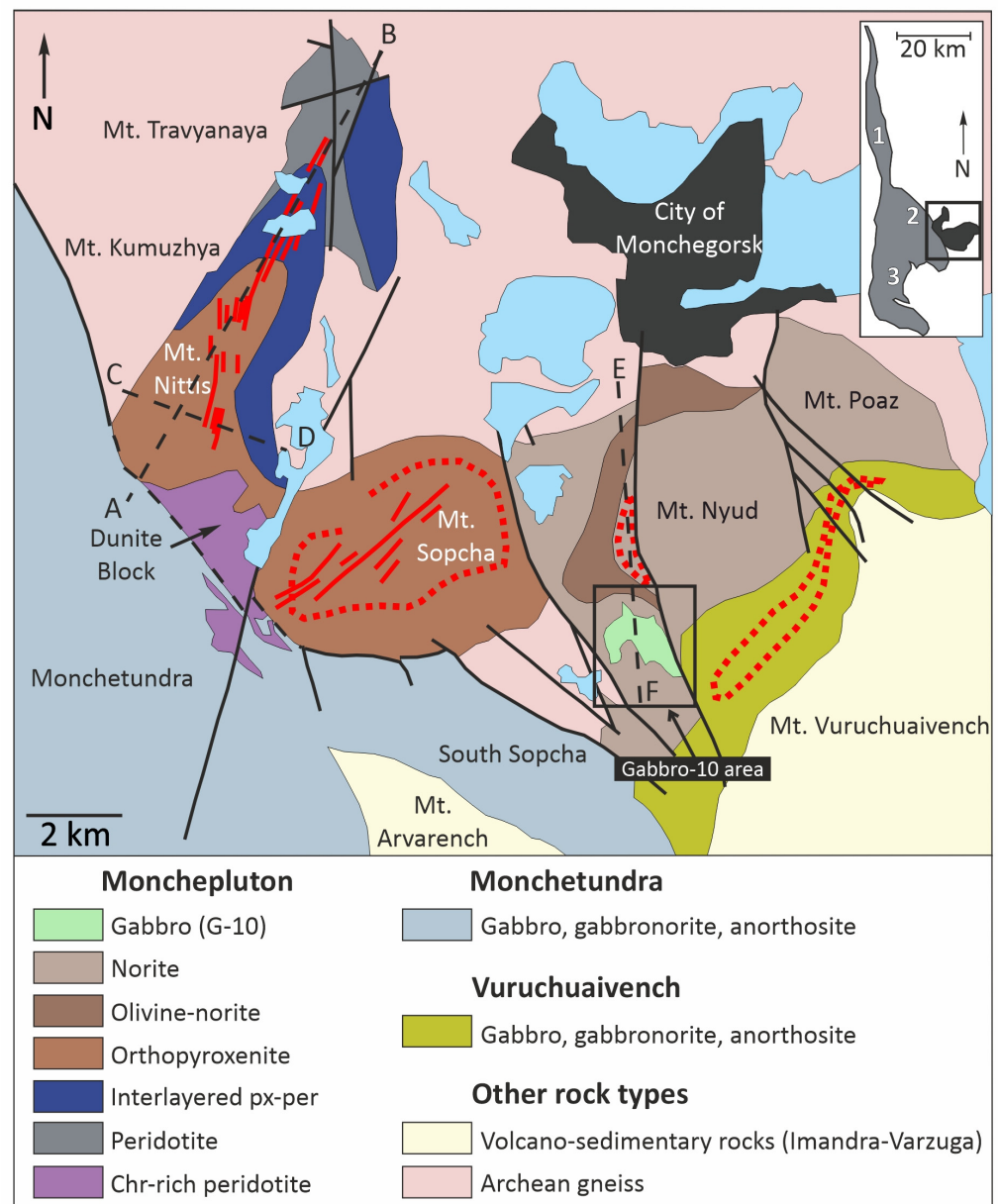


Figure 3. Schematic geologic map of the Monchegorsk Complex modified from [19,24]. Solid and dashed red lines show Cu-Ni-PGE sulfide mineralization. The inset shows the full extent of the Monchegorsk Complex, which includes the crescent-shaped Monchegorsk pluton (dark gray) and the elongated Main Ridge Complex (grey). Solid black lines are faults, dashed black lines correspond to geologic cross sections A–B, C–D and E–F. 1—Volchetundra, 2—Monchetundra, 3—Chunutundra. Abbreviations: chr—chromite, per—peridotite, px—pyroxenite.

3.1.1.1. NKT Massif

The NKT massif and the Sopcha massif adjacent to it (Figures 2–4) include ultramafic rocks of the lower Monchepluton zones: (1) the Peridotite zone is up to 500 m thick, including the Dunite block with chromitite layers; (2) the Interlayered Pyroxenite–Peridotite zone with a thickness of about 300 m; (3) the Pyroxenite zone with a thickness of more than 750 m [13]. The diverse sulfide mineralization of the NKT and Sopcha massifs includes contact-style PGE mineralization between host rocks and a trough-shaped lower part of the intrusion, reef-style mineralization in the Pyroxenite zone at Sopcha (330-ore layer), and vein bodies of massive sulfides. We are currently focused on the former (Figures 3 and 4).

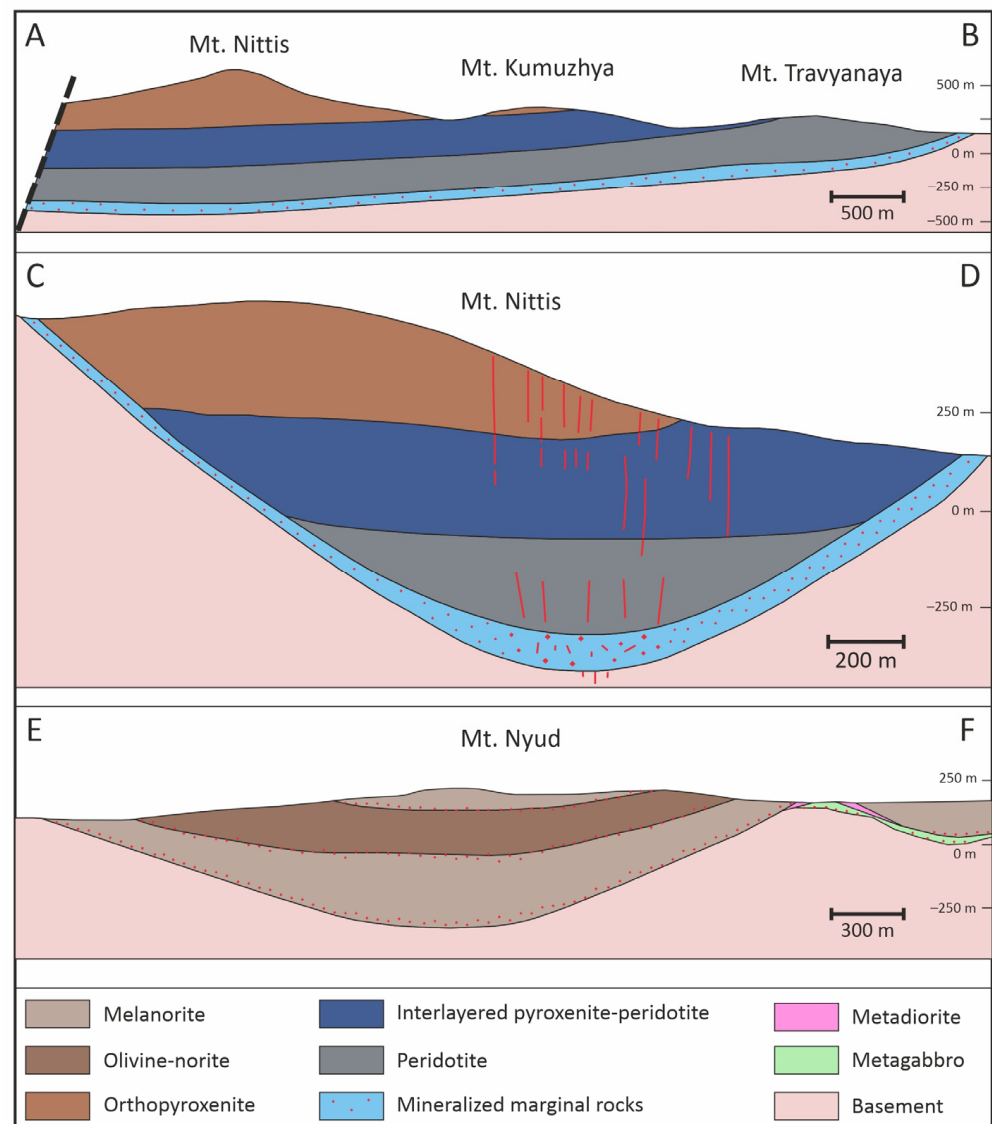


Figure 4. Simplified geologic cross sections along lines A–B (NKT intrusion), C–D (Nittis), and E–F (Nyud-Poaz intrusion) in Figure 3. Sulfide mineralization is shown in red, including massive sulfide veins (solid lines). Modified from [25].

Contact-style sulfide mineralization is dispersed in the marginal zone with a thickness of 20 m at the periphery to 200 m in the central part of the trough of the NKT massif. Sulfides are traced along the lower contact of the intrusion, covering, almost completely, the NKT and Sopcha massifs. The thickness of mineralization increases from peripheral to central parts of the intrusion, where it reaches 50 m with an average content of sulfides from 3 to 5 vol. %. Concentrations of Cu, Ni, Au, Pt, and Pd (ppm) in representative mineralized lithologies of the marginal zone are (1) 2225, 4265, 0.08, 0.27, and 2.81, respectively, in pyroxenites; (2) 2308, 3776, 0.04, 0.14, and 0.52 in gabbro-norites; and (3) 1071, 6476, 0.06, 0.15, and 2.81 in host metamorphosed sediments [13].

The genetic model of contact-style PGE mineralization of the NKT massif, based on detailed geochemical studies of the basal mineralized contact [13], relies on the following two key points. First, the geochemistry of chalcophile elements (Ni, Cu, PGE, Au) shows that all rocks overlying the mineralized zone contain cumulus sulfide ($Pt + Pd > 20$ ppb), indicating sulfur saturation of the magma in the intermediate chamber at depth and, consequently, effective accumulation of sulfide liquid in various portions of the marginal zone is the main ore-forming process. Second, efficient accumulation of sulfides is supposed to have

been facilitated by the long magmatic history of this block of the crust in the Paleoproterozoic, which began with preheating by smaller early intrusive phases or mafic–ultramafic dikes [26]. Thermal modeling (see next section) shows that, as a result of preheating, basement rocks become more susceptible to extensive partial melting, manifested as numerous felsic pegmatites near the contact, the source of volatiles added to the magma. Further, the added volatiles act as a flux, lowering the melting point of the cumulus minerals in the crystal mush. It leads to local small-scale dissolution of these cumulus phases within the mush and reduces the viscosity of the intercumulus melt, promoting gravitational settling of sulfide liquid (Figure 5).

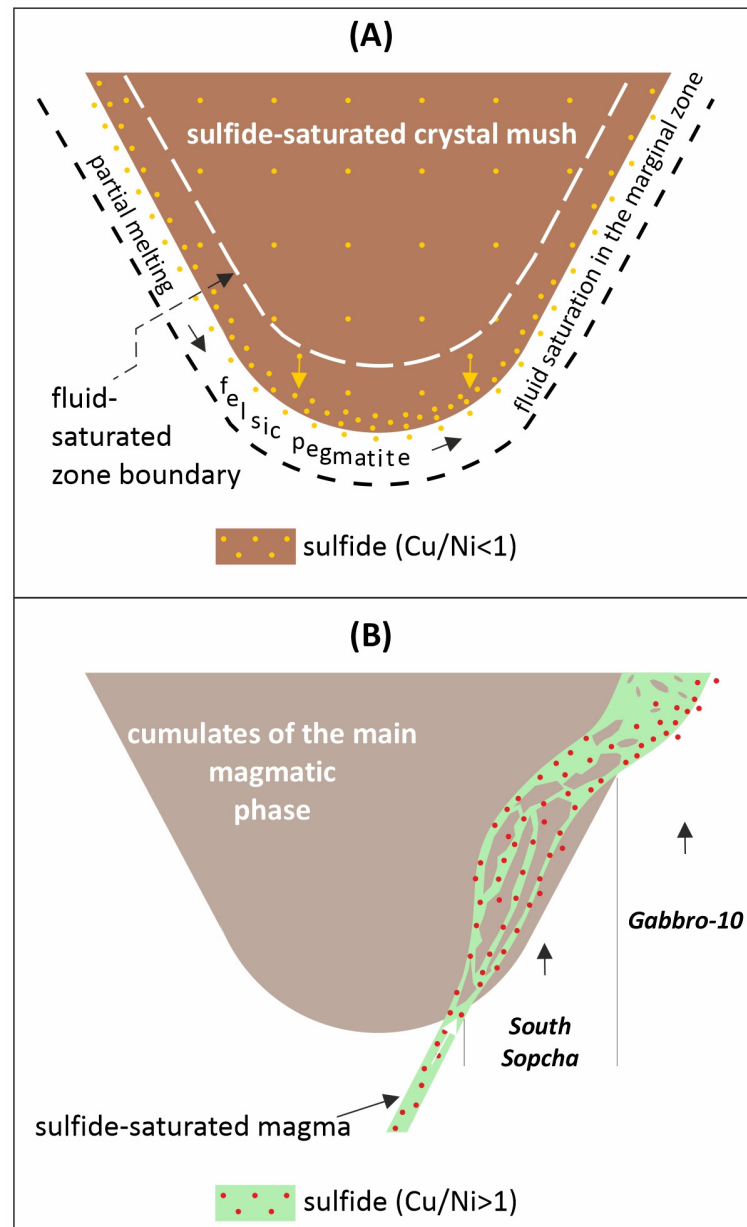


Figure 5. Schematic model for the formation of contact-style sulfide mineralization in the Monchegorsk pluton (Monchepluton). (A) As a result of basement preheating by early magmatic phases of smaller volume, the main phase has a significant partial melting halo, whose products, felsic pegmatites, introduce fluids into the near-contact zone of the main phase, reducing the viscosity of the intercumulus melt and increasing the infiltration capacity of cumulus sulfide within the fluid-saturated zone of crystal mush. (B) Late magmatic phases, smaller in volume and sulfide-saturated, form intrusive ore-bearing breccias (South Sopcha, Gabbro-10).

3.1.2. Thermal Modeling for the NKT Massif

The preheating of the basement was modeled taking into account an emplacement of several sills with a thickness of 50 m, spacing 250 m, at a depth of 2 to 4 km (Figure 6A). The intruding sills are assumed to have a temperature of 1200 °C [27]. Modeling shows that these thin sills cool relatively quickly, reaching temperatures below 800 °C after 10 years. It should be noted that basement temperatures above 700 °C are only reached in the immediate vicinity of the sills. However, these sills are capable of raising the average temperature of country rocks from less than 120 °C to more than 300 °C (Figure 6B).

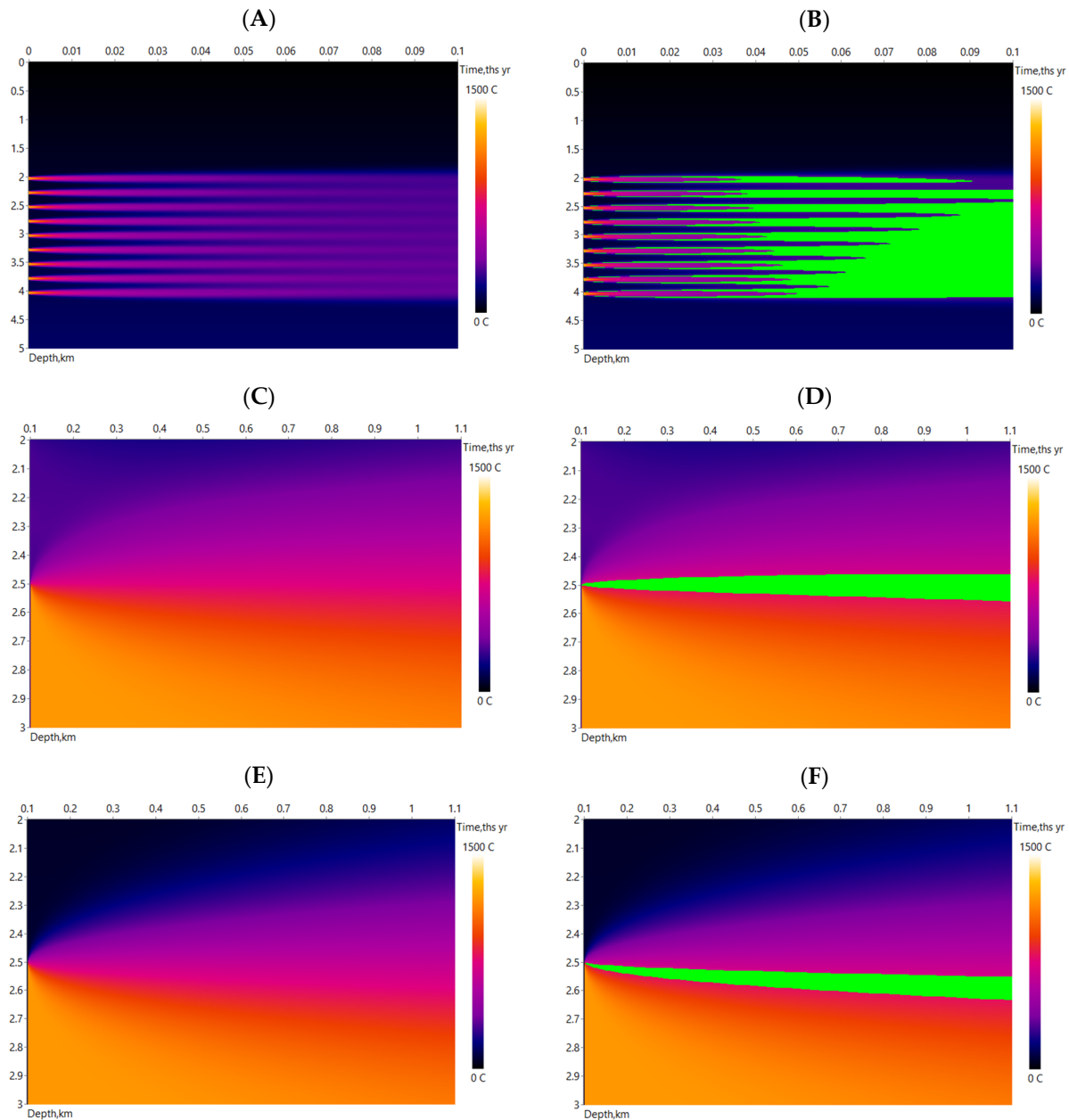


Figure 6. Thermograms for different emplacement scenarios of the NKT intrusion. (A,B) Preheating of the basement by a series of 50 m thick sills spaced 250 m apart. (C,D) Emplacement of a 1500 m thick crystal mush into preheated basement at a depth of 2.5 km. (E,F) Emplacement of a 1500 m thick crystal mush at a depth of 2.5 km into cold basement. The temperature ranges 300–400 °C (B) and 700–800 °C (D,F) are highlighted in green; magma/crystal mush temperature is 1200 °C. Note that a zone of significant partial melting (>700 °C) with a thickness of up to 36 m occurs only in the preheated basement.

At the second stage, it is assumed that the main pulse of magma that produced the NKT massif emplaced as a crystal mush with the same temperature into the preheated basement at a depth of 2.5 km (Figure 6C,D). The frequent occurrence of felsic pegmatites near intrusion contact strongly suggests partial basement melting, but dehydration melting requires temperatures above 700 °C [28]. The model shows that this temperature is reached up to several tens of meters from the intrusion contact after 100 years and even up to 80–90 m after 1000 years. Consequently, dehydration melting can also affect the distal portions of the basement if the latter has been preheated.

On the other hand, it can be assumed that the main impulse of magma was intruded into a cold basement, and all other conditions remained unchanged. Thermal modeling shows (Figure 6E,F) that basement temperatures above 700 °C can only be reached in close proximity to the intrusion contact at intrusion, which cannot explain the widespread development of pegmatite. Thereafter, the temperature gradually decreases from 700 °C, indicating much higher cooling rates compared to intrusion into a preheated basement (Figure 6F).

The model shows that an early emplacement of relatively thin sills can lead to significant preheating of the cold basement up to ~350 °C. Subsequent intrusions can then cause partial melting of the latter, producing abundant pegmatite, which would not be possible without basement preheating. Extensive dehydrative partial melting leads to saturation of the near-contact zone of the intrusion with fluids that lower the melting point of cumulus phases dispersed in the intruded magmatic mush. Due to the local melting of cumulus phases, the fluid-saturated zone, thus, receives a reduced viscosity of the intercumulus melt, which contributes to efficient accumulation of sulfide liquid near the lower contact.

3.1.3. Nude-Poaz Massif and Its Additional Phase Gabbro-10

Mafic–ultramafic rocks of the Nyud-Poaz massif, filling the continuation of the trough-like NKT massif in the east (Figure 3), belong to the ~450 m thick Norite zone of the Monchepluton. On the southeastern side of the Nyud-Poaz intrusion, its stratigraphy continues with metagabbro-norites of the Vuruchuaivench massif [29]. The norite Moroshkovoye Lake massif, an erosive remnant, is located about 1 km south of the Nyud-Poaz intrusion. The metamorphosed gabbroids between the Nyud-Poaz and Moroshkovoe Lake massifs contain norite xenoliths from these massifs [30] and are considered as an additional magmatic phase, complicating the lower contact and known as the Gabbro-10 intrusion [22].

The Nyud-Poaz massif and its satellites contain a variety of sulfide mineralization [31]: (1) sulfide dissemination along the lower contact; (2) sulfide horizons at the base and top of the olivine norite member, including lenses of massive sulfide at the top; (3) PGE reef in the Vuruchuaivench massif; (4) sulfide dissemination at the base of the Gabbro-10 intrusion. For the purposes of this study, the first is of interest, as in the case of the NKT massif and the last sulfide mineralization from the above list.

The mineralized horizon at the Nyud site is composed of sulfide-bearing melanorite overlying host tonalites with abundant veins and schlieren of felsic pegmatite, similar to that at the Nittis site. Mineralized melanorite gives way to a barren melanorite section without significant texture change. The content of visible sulfides is very similar to that in the NKT massif and is approximately 3 vol. %. Sulfides mostly occur as relatively small interstitial patches, up to 1 cm in diameter. Sulfides percolate, as in the NKT massif, from the mineralized marginal zone to basement rocks at a distance of up to 10 m. Concentrations of Cu, Ni, Au, Pt, and Pd (ppm) in representative mineralized lithologies are, respectively, (1) 18,993, 19,844, 0.13, 0.18, and 3.13 in melanorite and (2) 995, 2920, 0.02, 0.11, and 0.58 in tonalite [13]. The nickel nature of mineralization with a Cu/Ni ratio ≤ 1 should be noted.

Many common properties of the contact sulfide mineralization of the Nyud-Poaz massif and the NKT massif allow us to assume a similar formation model for the former, when, with the decisive role of basement preheating, sulfide liquid percolates through an interstitial melt of reduced viscosity due to the addition of fluid and partial melting of

cumulates in the near-contact zone. The presence of cumulus sulfide in melanorites of the Nyud-Poaz massif ($Pt + Pd > 20$ ppb) is traced for ~50 m from the lower contact [13].

The Gabbro-10 intrusion stratigraphy comprises two zones: (1) the Marginal zone and (2) the Gabbro zone (Figure 7). The Marginal zone, up to 10 m thick, is composed of fine- and medium-grained schistose metagabbros, geochemically similar to mesocratic gabbronorites [30]. The Gabbro zone consists of coarse-grained and medium-grained metagabbro, often characterized by a taxitic structure due to the alternation of rocks with different grain sizes. The average thickness of the Gabbro zone is 30–40 m. The geochemical composition of metagabbro corresponds to quartz meso-leucocratic gabbronorites. Metagabbro contains xenoliths up to 10×15 m in size. In terms of structural and textural features and geochemical composition, xenoliths correspond to melanorites of the Nyud-Poaz intrusion and its endocontact zone [30]. The metagabbro is overlain by the so-called metadiorite, at the base of which there is a layer of magnetite 1–2 m thick. As assumed in [22], the metagabbro and metadiorite are differentiates of the same intrusion, as evidenced by REE geochemistry, while, according to other assumptions, metadiorite can be considered as having an anatectic or metasomatic nature [32]. The U-Pb isotopic age of metagabbro 2497 ± 9 Ma (Supplementary Files) overlaps with the age of metadiorite 2498 ± 6 Ma [22], which coincides with an age of 2504 ± 2 Ma for the mafic pegmatite of the Nyud-Poaz intrusion [33]. Despite indistinguishable isotope ages at a given accuracy, the Gabbro-10 intrusion is clearly a late differentiated magmatic phase of the Monchepluton. Mineralized rocks containing from 1 to 5 vol. % of sulfides and localized near the lower contact are characterized by the following contents of Cu, Ni, Au, Pt, and Pd (ppm) in individual samples: (1) 3500, 1800, 0.07, 0.07, and 0.58 in schistose metagabbro, (2) 7700, 600, 0.12, 0.24, and 2.78 in metagabbro, and (3) 8000, 4400, 0.07, 0.46, and 2.28 in host tonalites [34]. It should be noted that all mineralized rocks of the Gabbro-10 intrusion are characterized by a predominance of copper over nickel.

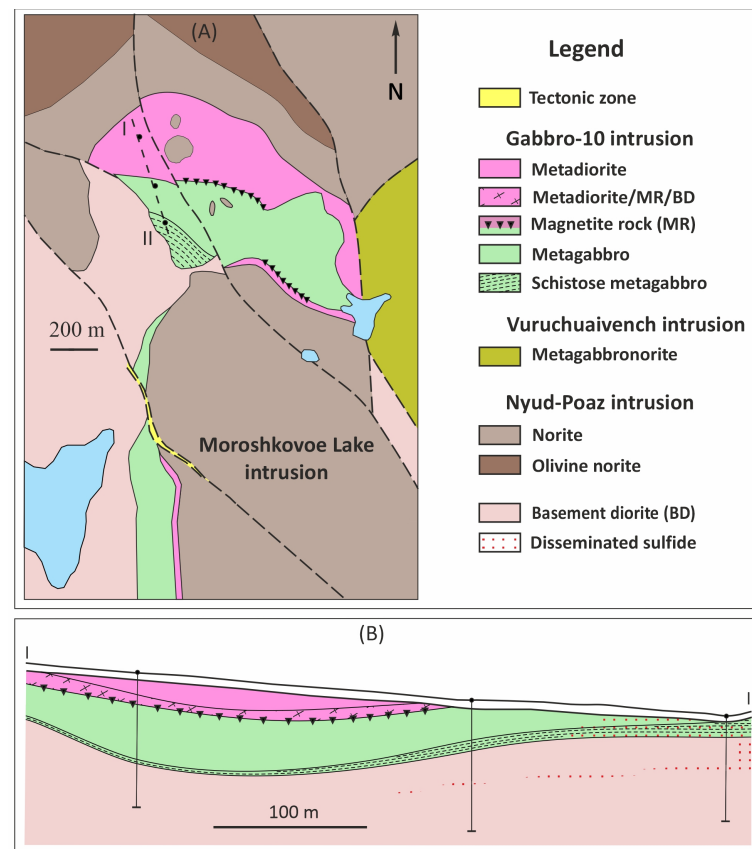


Figure 7. (A) Schematic geologic map of the Gabbro-10 intrusion. (B) Simplified geologic cross section, corresponding to profile I-II. Modified from [34].

Despite the high degree of secondary alteration of rocks in the Gabbro-10 intrusion, the similar position of mineralization near the lower contact suggests that the leading role in ore formation is held by the intercumulus spaces filled with a low-viscosity liquid, which, in turn, contributes to the formation of mineralization from sulfide-saturated crystal mush. As our model shows (Figure 8), the important difference here is that the preheating seems to have occurred not due to the emplacement of thin early magmatic phases but as a result of a significant thermal influence of the main intrusion. It is likely that the more developed seepage of sulfides into the basement rocks for the Gabbro-10 intrusion (up to 30 m; Figure 7B) compared to the NKT and Nyud-Poaz massifs is due to a higher degree of heating of the host rocks. Thus, the seepage of sulfides both through the crystal mush and the host tonalites determines the formation of mineralization, and in this regard, it can be assumed that without this process, sulfides would not have had the opportunity for accumulation. The last scenario (no mineralization) occurs when an additional intrusive phase (Gabbro-10) intrudes into the cooled contact of the Nyud-Poaz massif and can be characterized by thermal modeling to represent the maximum time gap between magmatic phases.

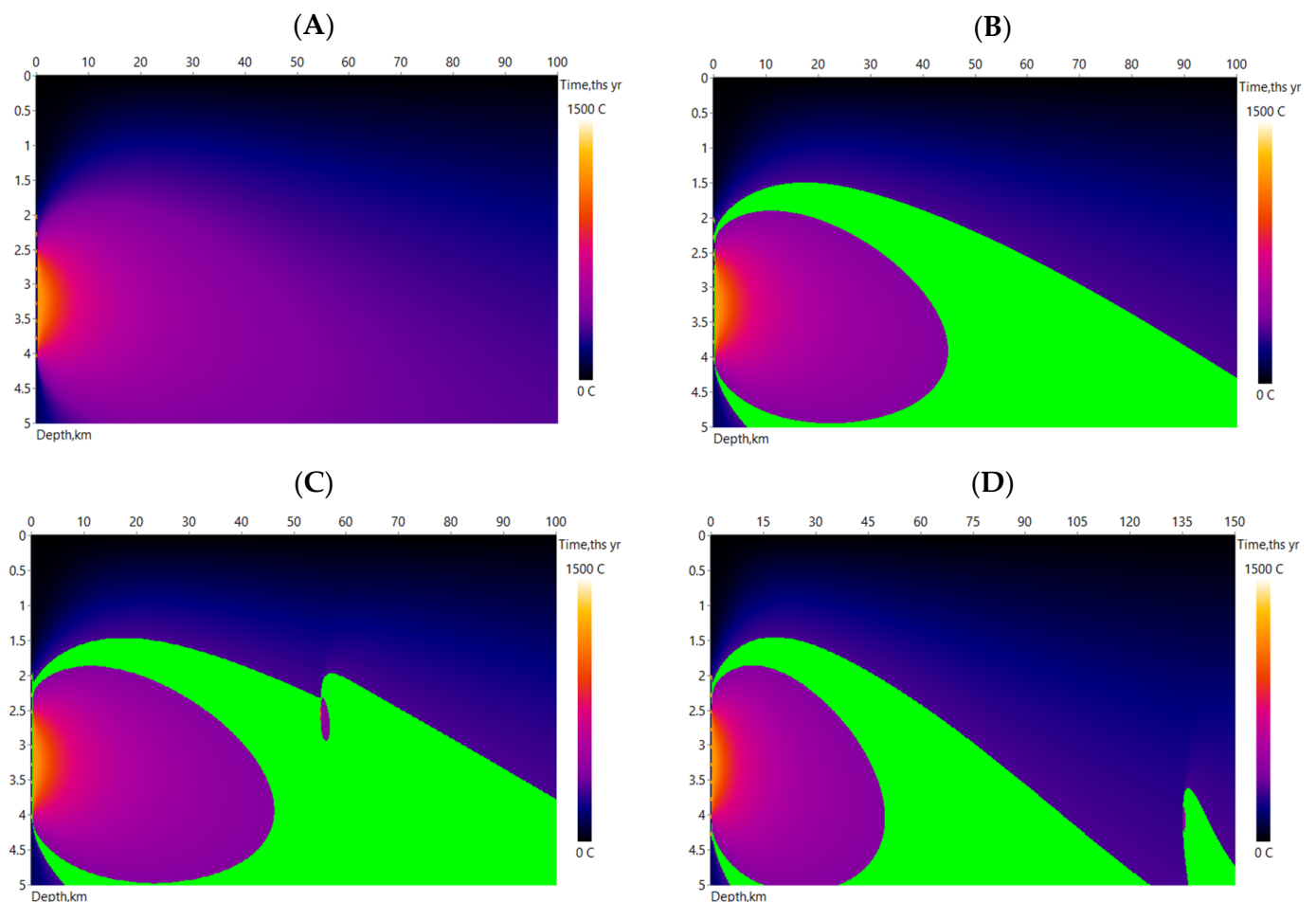


Figure 8. Thermograms for different emplacement scenarios of the Gabbro-10 intrusion. (A,B) Emplacement of a 1500 m thick main intrusive phase crystal mush into a preheated basement at a depth of 2.5 km. (C,D) Emplacement of a 50 m thick late intrusive phase into the upper ((C), favorable conditions for sulfide accumulation) or lower “thermal contact” ((D), sulfides stay dispersed within the late phase). The temperature range 300–400 °C is highlighted in green. See text for further explanation.

3.1.4. Estimation of the Time Gap between the Nyud-Poaz and Gabbro-10 Intrusions

The main magmatic phase of the Nyud-Poaz intrusion is modeled by a crystal mush 1500 m thick body with a temperature of 1200 °C, which was intruded at a depth of 2.5 km (Figure 8A). An additional phase represented by the Gabbro-10 intrusion is shown in Figure 8C (upper “thermal contact”) and Figure 8D (lower “thermal contact”) in the form of a magmatic 50 m thick body with the same temperature. In Figure 8B, a region with temperatures from 300 to 400 °C is highlighted, corresponding to the preheating volume. Comparing Figure 8C,D, one can see that a favorable scenario for the formation of sulfide mineralization in the Gabbro-10 intrusion is shown for the case of emplacement in the upper “thermal contact” in Figure 8C. Modeling shows that saving favorable conditions for sulfide percolation, the maximum time gap will occur on the lower “thermal contact” at a depth of 4 km (Figure 8D) and will be ~100 ka. Unfortunately, with the state-of-the-art accuracy of isotope studies [35], this time gap cannot be estimated using geochronological methods, which is emphasized by the obtained ages of the Nyud-Poaz and Gabbro-10 massifs, being indistinguishable within the error [22,33].

3.2. Fedorova–Pana Complex

The Paleoproterozoic Fedorova–Pana Complex (Figure 2), formed at the same time as the Monchegorsk Complex, is located in the central part of the Kola Peninsula and characterized by a variety of sulfide mineralization, including PGE reefs in the central portions of intrusions and contact-style mineralization at the base [36–38]. The Fedorova–Pana Complex consists of three main layered intrusions of predominantly mafic composition: Fedorova, West Pana, and East Pana. Details of the geology for each of these intrusions are available in the following references [39–41]. The Fedorova intrusion is the western part of the complex and hosts the largest PGE deposit in Europe, which can be compared, e.g., with the Suhanko deposit in Finland [7].

3.2.1. Fedorova Intrusion

The Fedorova intrusion forms a lenticular 4 km thick body, dipping steeply to the southwest (Figure 9A). In the stratigraphy of the Fedorova intrusion, three zones are distinguished from bottom to top: (1) Norite-Gabbronorite zone (or “basal unit”), (2) Leucogabbro-Gabbronorite zone, and (3) Leucogabbro zone [42]. It is assumed that the Leucogabbro-Gabbronorite and Leucogabbro zones constitute an early magmatic phase (2526–2515 Ma) with reef-style PGE mineralization, while the basal unit hosting economic contact-style PGE mineralization belongs to a later intrusive phase with ages in the range of 2493–2485 Ma [36,37,43]. The basal unit, 300 m thick, is composed of inequigranular melanorite and gabbronorite containing abundant barren orthopyroxenite autoliths and irregular patches of disseminated PGE-enriched sulfides ranging from 2 to 5 vol. % (Figure 9B). Uniformly disseminated sulfide accumulations (20–30 vol. %) occur as single finds, and massive sulfides are absent. Averaged concentrations of Cu, Ni, Au, Pt, and Pd (ppm) in mineralized rocks are 1200, 800, 0.08, 0.29, and 1.2, respectively [36]. Sulfide mineralization is confined only to the basal unit and shows no signs of sulfide liquid percolation into the basement rocks. This sulfide mineralization forms the Fedorova Tundra Cu-Ni-PGE deposit with total PGE reserves of about 400 t [8].

It is believed that the first intrusive phase of the Fedorova intrusion preheated the basement before emplacement of the second phase along the lower contact of the first intrusive phase (Figure 9). The thermal contact halo of the first phase exceeds 100 m, as evidenced by partially remelted two-pyroxene diorites observed in some drillholes [40]. Despite this, the second intrusive phase shows little evidence of sulfide accumulation within the basal unit or sulfide percolation into basement rocks. Therefore, the time gap between intrusive phases was long enough to cool the basement below 300–400 °C (basement temperature supporting migration and accumulation of sulfides dispersed within crystal mush, as follows from the model for the NKT intrusion; see above).

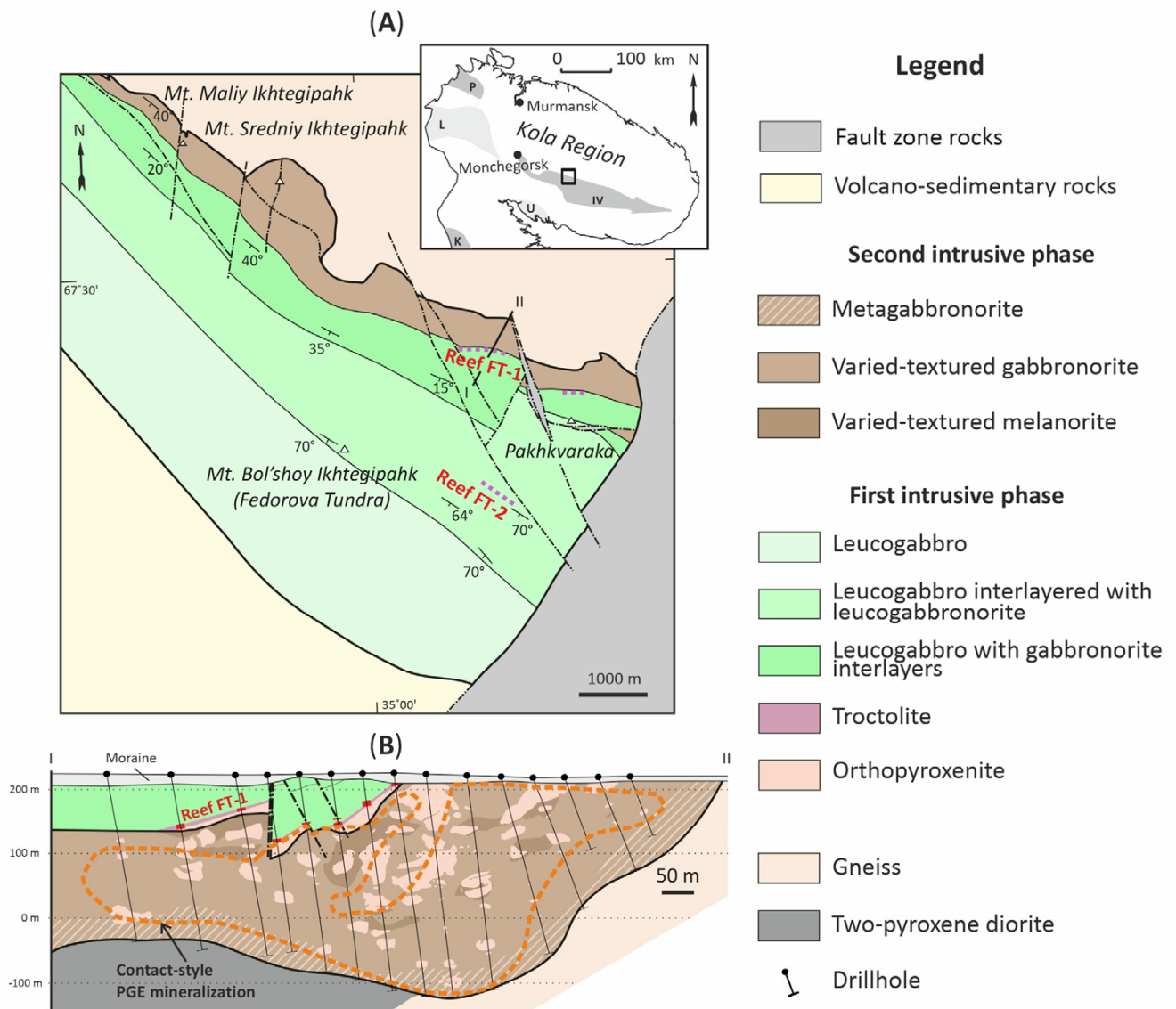


Figure 9. (A) Schematic geologic map of the Fedorova intrusion. (B) Simplified geologic cross section, corresponding to profile I-II. Modified from [36].

3.2.2. Estimation of the Time Gap between the Magmatic Phases of the Fedorova Intrusion

U-Pb isotope zircon dating from magmatic phases of the Fedorova intrusion shows that the pyroxenite from the first phase has an ID-TIMS age of 2526 ± 6 Ma, which is about 40 Ma older than the U-Pb age of the ore-bearing 2485 ± 9 Ma gabbro [43]. There is no doubt that these data can be refined by searching for more reliable points for calculating the age, since all published ages of the Fedorova rocks do not contain a single point on concordia. The first results of local U-Pb SHRIMP-II dating of zircon from ore-bearing gabbro show an age of 2491 ± 6 Ma and contain three concordant zircon grains (sample FT-21-1, Supplementary Files), confirming the isotope age of the second magmatic phase. In this regard, the thermal assessment of the minimum time gap between magmatic phases, by analogy with the Gabbro-10 intrusion, is of particular interest.

Thermal modeling shows that the emplacement of the first phase presented by crystal mush with a temperature 1200 °C leads to significant heating of the underlying rocks (Figure 10). The temperature of partial melting of the basement (~ 700 °C) can extend to a distance of ~ 90 m from the lower intrusion contact in 20–25 ka (Figure 10A,B). This is consistent with the thickness of two-pyroxene diorites below the intrusion [40].

Since the magma of the second intrusive phase was likely sulfide-saturated [37], as a result of its emplacement into the contact with the basement heated by the first phase, sulfides should have been concentrated near the base of the intrusion, forming sulfide-enriched layers and percolating in places into the Archean gneiss basement. Figure 9B shows that sulfides are unevenly distributed across the whole 300 m thick basal unit of the Fedorova intrusion, and no migration of sulfide liquid is observed. Consequently, the basal unit, consisting of varied-textured gabbro-norites postdating the first intrusive phase, intruding after the temperature at the lower first phase contact dropped below 300 °C. Under these boundary conditions, the minimum time separating different intrusive phases is about 650–700 ka, as seen in Figure 10C,D. Taking into account these estimations and a state-of-the-art accuracy of U-Pb geochronology, which is ± 300 ka [35], the question of the duration of the Fedorova intrusion crystallization can be considered at the next accuracy level.

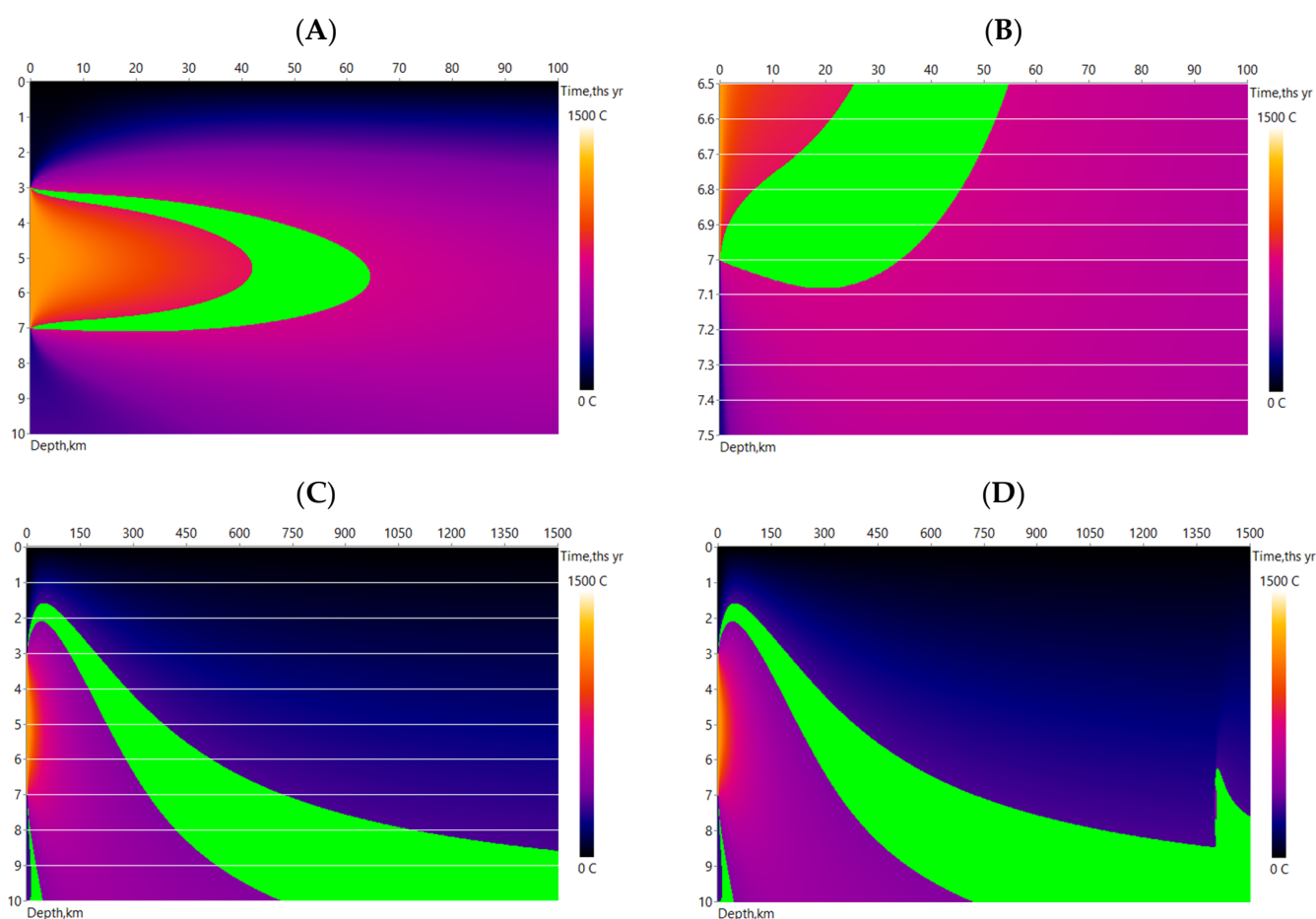


Figure 10. Thermograms for the two-phase emplacement of the Fedorova intrusion. (A) Emplacement of crystal mush of the main intrusive 4000 m thick phase into a cold basement at a depth of 3 km. (B) Time–depth–temperature profile for 700–800 °C in the area of the lower contact of the main phase. Noted that the zone of basement partial melting is almost 100 m thick. (C) The rate of cooling of the basement heated as a result of the main phase emplacement. (D) Emplacement of the late 300 m thick intrusive phase crystal mush at the lower contact of the main phase. The temperature ranges 700–800 °C (A,B) and 300–400 °C (C,D) are highlighted in green. See text for further explanation.

4. Discussion

4.1. A Moment of Sulfur Saturation

The main point of the debates regarding the origin of PGE-enriched sulfide mineralization is the moment of sulfur saturation in the magma, when the sulfide liquid immiscible

with the silicate melt begins to extract base and precious metals from the magma [1]. It should be noted that the efficiency of this process is determined by the high values of PGE distribution coefficients for coexisting silicate and sulfide liquids, reaching, for example, 1000 for copper and 30,000 for palladium [44]. One can expect the following products of evolution for a system of the magma undergone sulfur-saturation: (1) cumulates formed before sulfur saturation; (2) accumulations of sulfides with PGE; (3) sulfides dispersed in cumulates; (4) cumulates depleted in PGE as a result of the interaction of sulfide and silicate liquids. Among the ore-bearing layered intrusions of the eastern part of the Fennoscandian Shield, located mainly in the Kola region, only the presence of PGE mineralization and dispersed sulfides is indisputable.

The geochemistry of chalcophile elements indicates that the rocks of the Dunite block in the Monchegorsk pluton, which do not contain cumulus sulfides, may be results of crystallization from sulfur-undersaturated magma [13]. However, the Dunite Block is believed to be a giant xenolith and a product of an early high-magnesian magma that does not contain gradual transitions to the predominant rocks of the pluton with cumulus sulfides ($Pt + Pd > 20$ ppb) formed from sulfur-saturated magma. Thus, in the magma chamber of the Monchegorsk pluton on the surface, we observe the result of sulfur saturation that occurred in the system (rocks with and without cumulus sulfide). But, the immediate moment of sulfur saturation cannot be seen, because it apparently occurred in a staging chamber at depth.

The formation of contact-style PGE mineralization is often considered in the context of the genesis of extended PGE reefs in the central portions of intrusions. Grobler and colleagues [5], for example, established a stratigraphic correlation between the Merensky Reef in the Critical Zone and the Platreef, located at the contact of the Bushveld Complex with country rocks. Iljina considered the Siika-Kama Reef and the contact-style deposits Sukhanko and Kontiyarvi as elements of the ore-magmatic system of a single “Portimo Reef” [7]. Quite characteristically, some classical reefs, such as the Merensky Reef and J-M reef, are overlain by depleted in PGE rocks [1], indicating sulfur saturation occurring directly in the chamber. It should be noted that nothing of the kind is observed in the Sopcha Reef (330 ore bed) and Vuruchuavench Reef at Monchegorsk [21], suggesting the intrusion of mineralized units as sills of magma that experienced sulfur saturation and PGE enrichment at depth. Since the “deep character” of sulfide saturation is also assumed for formational models of reef- and contact-style PGE mineralizations of the Fedorova–Pana Complex, the search for key ore-forming processes for contact-style mineralization in the Kola region should be focused on two main factors: emplacement of sulfide-saturated magma and gravity.

4.2. Emplacement of Sulfur-Saturated Magma and Gravity

A consideration of the contact-style PGE mineralization of the Kola region from the point of view of the ratio of these factors is provided below. On the one hand, in the section of the typical ore-bearing layered intrusion, the Monchegorsk pluton, according to the model presented for the first time by Karykowski and others [13] and described above, both the intrusion of cumulus sulfide-enriched magma and gravity play a significant role. The gravity effect on the example of the NKT intrusion is not quite obvious at first glance, since sulfides form predominantly interstitial dissemination without a wide development of sulfide droplets. In this regard, it is important to take into account the state of the intruding material, which, apparently, corresponded to a sulfur-saturated and crystal-rich magma or crystal mush. When studying the drillhole section of the Pyroxenite zone in the NKT intrusion, it turned out that the magnesian number of cumulus orthopyroxene gradually, over ~200 m, decreases from 86 to 84 mol. % towards the contact together with MgO and Cr/V decreasing. A possible explanation for this decrease is the balancing of the orthopyroxene composition with intercumulus melt, the amount of which increases towards the contact due to partial melting of cumulus minerals caused by a decrease in their melting temperature as a result of the addition of fluid to the system. Fluid input

can be provided by extensive dehydration partial melting of country rocks, which can be achieved if basement rocks are preheated by the intrusion of small early intrusive phases, as shown through thermal modeling. A newly formed intercumulus melt, thus, acquires a reduced viscosity and provides an increased porosity of the crystal mush, through which sulfides seep into the rocks of the marginal zone and into the Archean basement under the gravity influence.

On the other hand, in the same Monchegorsk Complex, there are several examples of platinum–metal mineralization located near the contact with the basement. To understand this, it is necessary to accept an unusual fact for the classical theory of crystallization of layered intrusions. Namely, the marginal zones of layered massifs are favorable for placing additional magmatic injections, including ore-bearing ones. In the Monchegorsk Complex, such ore-bearing injections, apparently, are a series of vein bodies of mineralized taxitic norites and gabbronorites in the South Sopcha intrusion and mineralized metagabbro in the Gabbro-10 intrusion. At the same time, imagining the development of the process of emplacement of vein taxitic gabbronorites cutting the orthopyroxenites of the South Sopcha massif, it is easy to see the pattern of intrusive breccia at the base of the Fedorova intrusion (Figure 9B), which can already be considered as a separate late intrusive phase. The time gap between the late and main intrusive phases, as shown through thermal modeling, may determine whether the gravitational factor will determine ore formation (Gabbro-10) or not (Fedorova Tundra). In this regard, in the series of examples listed above, the factor of additional intrusion of ore-bearing magma comes to the fore and allows us to consider these mineralized rocks as an individual (intrusive) variety of contact-style PGE mineralization.

4.3. Thermal Modeling of a High-Temperature Progressive Facies of Metamorphism in the Contact Halo of Ore-Bearing Intrusions in the Norilsk Region

The mathematical model used in this paper limits the characterization of the considered intrusive complexes to only the thermal component, unlike the known modelling software [45,46]. In fact, intrusive bodies being emplaced are modeled by simultaneous heating of the host rocks at different times. In our opinion, the narrow focus of the model can be an advantage and figuratively compared with seismic–acoustic studies that extract valuable geologic information from only one characteristic of the propagation of elastic waves in different rock units. At the same time, interpretation of the obtained data, namely, temperature ranges corresponding to the melting and heating zones, can indirectly give an idea of the possible time scenarios for the formation of sulfide Cu–Ni–PGE mineralization in mafic–ultramafic complexes and contribute to the formulation or testing of a genetic hypothesis.

The mathematical model, however, allows us to consider such a parameter as the duration of the hot magma flow, which is provided for in the Gehenna 2.2 program presented here and implemented by stopping the cooling of the intruded strata according to the heat transfer equation. An excellent example of the importance of the magma flow duration for ore generation is the Norilsk ore-bearing intrusions [47]. It is well known that the Norilsk ore-bearing intrusions, located in the north of Siberia, are elements of the plumbing system for Permian–Triassic trap basalts. According to A. Naldrett, the volume of hot magma that has passed through the “main bodies” of intrusions (Figure 11A) is many-times greater than the volume of the intrusions themselves [1]. Long-term magma flow and crystallization of intrusions led to the development of an anomalous contact-metasomatic aureole, the thickness of which is comparable to the size of the ore-bearing intrusions and reaches 200 m. Detailed studies by D.M. Turovtsev showed [48] that the contact aureoles of the Kharaelakh and Talnakh intrusions, located in Devonian sedimentary rocks, consist of approximately equally developed progressive and regressive facies of contact metamorphism. At the same time, the thickness of the highest-temperature facies of pyroxene hornfels (900 °C) is approximately half the thickness of the contact-metasomatic aureole (Figure 11B). Knowing the thickness and temperature of the formation of the aureole, as well as the temperature of the magma, we can calculate the duration of the flow

process, determining the time frame for the dynamic development of these complex ore-magmatic systems. Thermal modeling for the Norilsk intrusions, e.g., for the Kharaelakh intrusion [1], can be divided into three stages: (1) preheating of country rocks, (2) intrusion of a “peripheral sill”, and (3) formation of the “main body” of the intrusion within the sill.

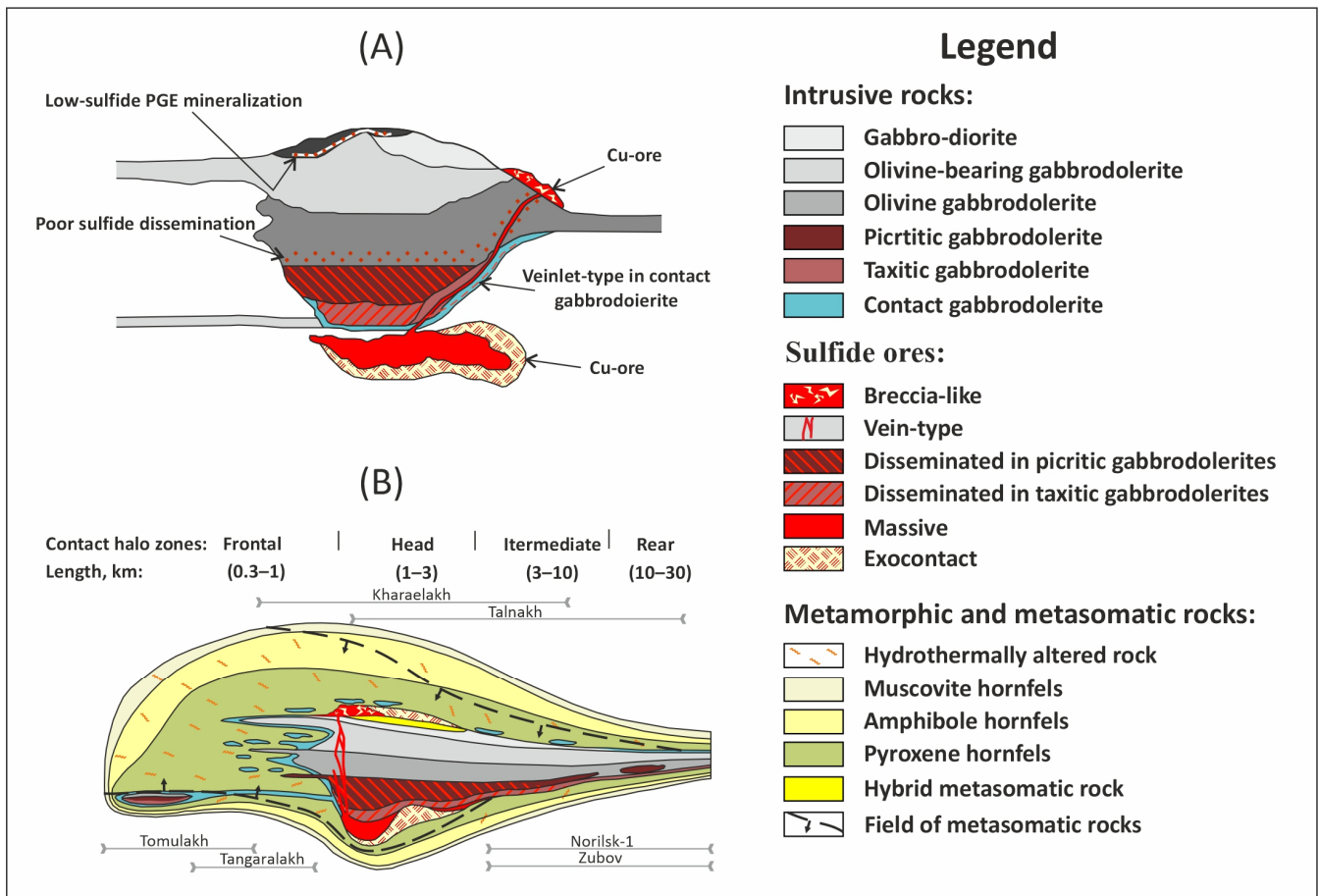


Figure 11. Geology of the Norilsk ore-bearing intrusions according to models from A. Naldrett (A) and D.M. Turovtsev (B). Modified from [1,48].

Stage 1: preheating of country rocks. As a probable preheating scenario, successive intrusion and cooling of seven magma sills with a thickness of 20 m and a temperature of 1300 °C are used with an interval of 10 years. The sills are located every 100 m at a depth interval of 2.7–3.3 km (Figure 12A). As a result, a zone of elevated temperatures (for example, more than 300 °C) is formed and exists for more than 0.5 ka (Figure 12B). In view of the initial stage of trap magmatism, during which intrusions were emplaced, it is important to take into account the preheating of host rocks, since, firstly, it affects the size of the final thermal aureole, increasing it by a few tens of meters, and, secondly, as shown above, preheating is essential for the formation of sulfide accumulations at intrusion contacts.

Stage 2: “peripheral sill” emplacement. A peripheral sill, understood as a part of the Norilsk-type intrusion, connected with the main body and not having the petrographic diversity and accumulations of massive sulfide ores inherent in the main body, is modeled by the simultaneous intrusion of magma 50 m thick at a depth of 3 km, which begins to cool immediately after intrusion in the area of preliminary heating without forming a contact halo outside its limits (Figure 12C). This is consistent with our geological observations, indicating an almost complete absence of contact alteration of rocks in peripheral sills, represented, for example, by the South Norilsk intrusion [49].

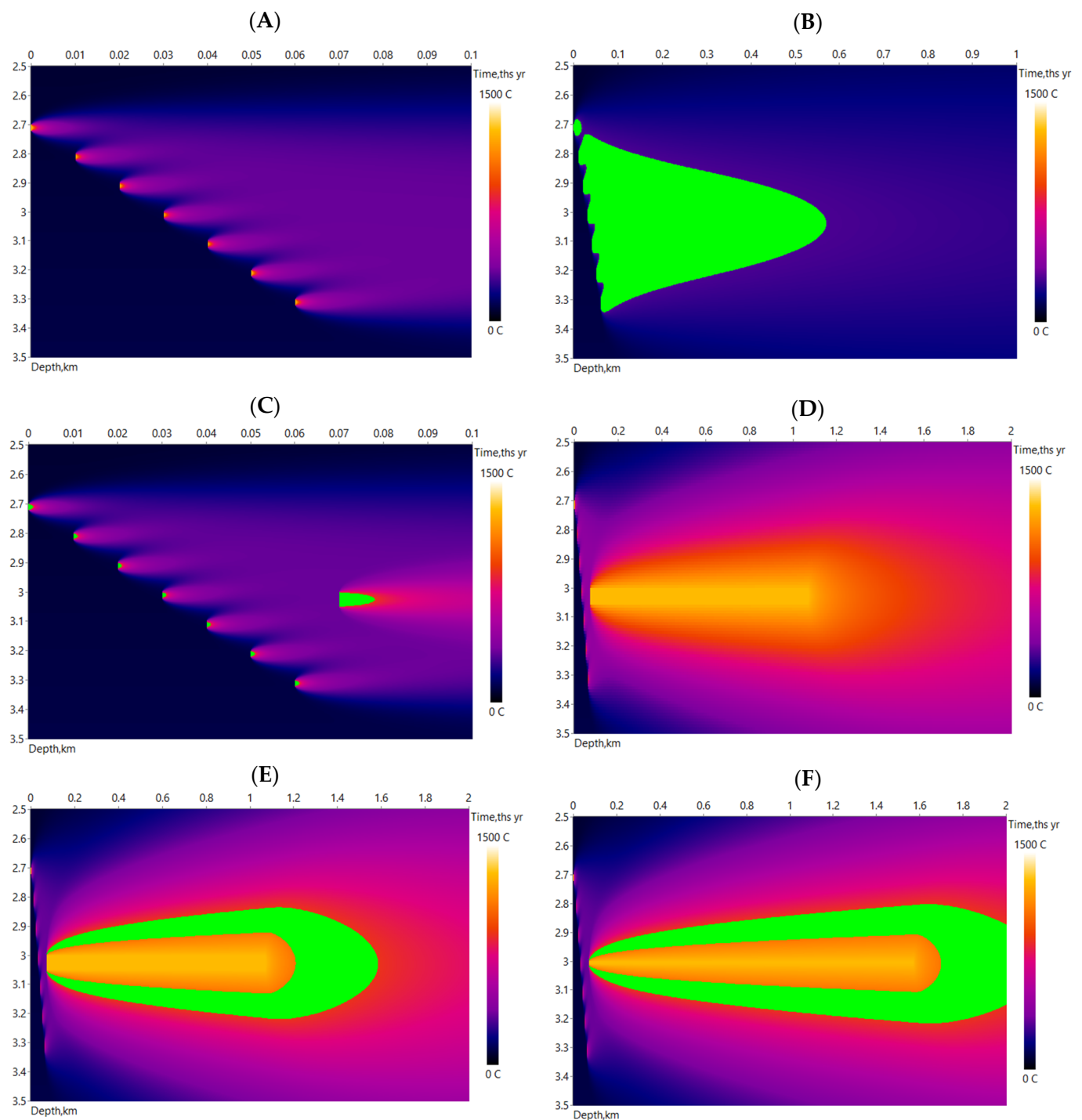


Figure 12. Thermograms for different stages of the Norilsk ore-bearing intrusions formation. (A,B) Stage 1: successive emplacement of a series of magma 20 m thick sills having temperature of 1300 °C at depths from 2.7 to 3.3 km. (C) Stage 2: intrusion of a 50 m thick magma sill into preheated country rocks at a depth of 3 km. (D,E) Stage 3: formation of the “main body” and surrounding contact aureole due to the continuous flow of magma with a temperature of 1300 °C inside a 50 m thick sill for 1000 years. (F) Same as option E inside a 10 m thick sill over 1500 years with a resulting intrusion thickness of 203 m and an upper hornfels halo of 102 m. The area in green is over 300 °C (B), over 900 °C (C) and within a range of 900–1100 °C (E,F). See text for further explanation.

Stage 3: “main body” formation. In agreement with one of the scenarios for the formation of the main bodies and associated sulfide ores, which assumes the passage through them of a volume of magma that is several orders of magnitude greater than their observed volume [1], emplacement of the peripheral sill is further complicated by the long-term flow of magma inside it. According to calculations, the flow of magma with a temperature of 1300 °C inside a 50 m thick channel for one year leads to the formation of a “hornfels zone” ($T > 900$ °C) with a thickness of about 6 m, which increases with the time of magma flow to 20 and 60 m over periods of 10 and 100 years, respectively. In the latter case, with the growth of the hornfelsing halo, the zone of complete melting of the host rocks will grow, which in 100 years, will reach 30 m from the initial upper and lower contacts of the sill. The molten and dissolved matter of the host rocks ($T > 1100$ °C) is removed from the main body due to the flow of magma that forms a channel 110 m thick over 100 years with hornfelsing haloes of 30 m on each side of the intrusion. Further continuous flow of magma leads to the expansion of the zone of contact changes in rocks, which is accompanied by an increase in the melting zone and, hence, the thickness of the intrusion, which ultimately makes it possible to obtain the desired ratio of the thickness of the main body and the hornfelsing halo. For example, after 1000 years of magma flow, a channel with a thickness of about 200 m and a halo of half the thickness are formed (Figure 12D,E), which was required to show.

Numeric simulations confirm that the open, dynamic, and long-term nature of magma emplacement is the determining factor for the ore–magmatic system of the Norilsk intrusions. This is also indicated by the presence of eruptive breccias, which testify to the multiphase intrusion, the large thickness of massive sulfide bodies [50], the facies variability in ore-bearing intrusions [51], and the structural and textural features of the most important stratigraphic units of intrusions [52]. The horizons of picritic and so-called upper taxitic gabbrodolerites [53] are a unique example of a system where the fluid, introduced into a subhorizontally moving magma, provided a subvertical redistribution of sulfide liquid in it due to surface tension forces with extreme PGE enrichment in the upper part containing oxide–sulfide–silicate–fluid foam [52,54]. Taking into account the thickness of the picritic and upper taxite gabbrodolerites, it is worth noting that the thickness of the long-term magma flow within the intrusive bodies was probably well below the 50 m suggested by our original scenario (Figure 12E). In Figure 12F, it can be seen that the 10 m flow is also able to form the “main body” and the accompanying contact aureole of pyroxene hornfelses in 1500 years.

We are far from thinking that the modeling performed can put a decisive end to the long-term discussion about the origin of the stratification and the unique metal endowment of the ore-bearing intrusions of the Norilsk region. However, we hope that such an approach and the presented software, due to its simplicity, can be very useful in developing scenarios for the formation of both specific intrusions or their parts and the Norilsk ore region as a whole. Many intrusions with disseminated sulfides are known near Norilsk [51], but they are not interesting for industry at the moment with the ongoing mining of massive sulfides.

5. Conclusions

In the example of the ore-bearing intrusions of the Monchegorsk and Fedorova–Pana complexes in the Kola region, as well as the example of the Norilsk intrusions in the north of the Siberian Platform, it is shown that the following geological processes can be attributed to the key ones: pulsating long-term magmatism, preheating of country rocks, and gravitational settling of sulfide liquid in the lower parts of intrusions with sulfide liquid migration into host rocks, up to their complete replacement by sulfides (Norilsk deposits).

Consideration of the thermal history for sulfide-bearing intrusions of the Monchegorsk and Fedorova–Pana complexes allows us to draw the following conclusions regarding the formation of contact-style Cu–Ni–PGE mineralization presented by disseminated sulfides.

1. The key role for the concentration of sulfides in the lower parts of intrusions belongs to preliminary heating of the host rocks by early magmatic phases of a smaller volume.

It is a necessary condition for the appearance of a significant halo of partial melting around the main magmatic phase. Its products, represented by felsic pegmatites, bring fluids into the near-contact zone of the main phase, reducing intercumulus melt viscosity and increasing the infiltration capacity of the cumulus sulfide (NKT, Sopcha, Nyud-Poaz).

2. In the presence of late ore-bearing magmatic phases of a relatively small volume, the pattern of sulfide distribution along the smaller phase can be used to estimate the time gap with the main phase. Thermal modeling shows that the Gabbro-10 intrusion, an additional ore-bearing phase of the Nyud-Poaz massif, is separated from the main phase by a time gap of no more than 100 ka, while the minimum gap between the magmatic phases of the Fedorova intrusion is 650–700 ka.

In addition, the development of hornfels aureoles around mafic–ultramafic rocks makes it possible to estimate the duration of the process of continuous magma flow inside intrusions, which, as an example from the Norilsk ore region shows, can reach 1000 years and more.

Thus, 1D thermal modeling data can be used both for formulating genetic hypotheses and testing various scenarios of the formation of sulfide Cu-Ni-PGE mineralization in mafic–ultramafic complexes. It should be emphasized that the calculation results presented in this article are numerical models and are intended for use in the field of economic geology. The following issues can be proposed as interesting topics for further tests using the Gehenna 2.2 software: (1) numerical estimation of the lower limits of the duration of the formation of the Stillwater Complex after the thickness of the underlying hornfels; (2) comparison of the thermal history between the Paleoproterozoic West Pana intrusion, which caused only partial melting of Archean alkaline granites, and the Stillwater Complex surrounded by a thick hornfels halo; (3) lower limits assessment for the magma flow duration while the formation of erosion depressions (potholes) within the underlying cumulates below PGE reefs.

Supplementary Materials: The following supporting information can be downloaded at: <https://www.mdpi.com/article/10.3390/min13081046/s1>, (1) Gehenna 2.2. software zip-file with tables of input parameters; (2) SHRIMP U–Pb isotope data for zircon from the metagabbro of the MC and from the taxitic gabbro-norite of the FPC.

Author Contributions: Conceptualization, D.S. and N.G.; methodology, N.G.; software, D.S.; writing—original draft preparation, N.G.; writing—review and editing, D.S.; funding acquisition, N.G. All authors have read and agreed to the published version of the manuscript.

Funding: This research was funded by the Russian Science Foundation (RSF), grant number 22-27-20106, <https://rscf.ru/project/22-27-20106/>, accessed on 1 January 2023.

Data Availability Statement: The data presented in this study are available in Supplementary Materials.

Acknowledgments: The idea to write a software for thermal modeling came from our joint work with Bartosz Karykowski under the Monchegorsk sulfide mineralization theme. Discussion of various aspects of the Norilsk region geology with A.G. Pilyugin, V.A. Radko and E.M. Spiridonov was useful for the reconstruction of its thermal history. The starting point for consideration of the formation of Triassic intrusions was the joint work with I.I. Nikulin, Yu.A. Mikhailova, A.O. Kalashnikov, Ya.A. Pakhomovsky and R.I. Kadyrov on the project “Identification of the relationship between the structural-textural and material properties of sulfide copper-nickel ores”. The authors are grateful to A.N. Ivanov and A.M. Sushchenko for their help with illustrations.

Conflicts of Interest: The authors declare no conflict of interest.

References

1. Naldrett, A.J. *Magmatic Sulfide Deposits: Geology, Geochemistry and Exploration*; Springer: Berlin, Germany, 2004; p. 488.
2. Barnes, S.-J.; Lightfoot, P.C. Formation of Magmatic Nickel Sulfide Deposits and Processes Affecting Their Copper and Platinum Group Element Contents. In *One Hundredth Anniversary Volume*; Society of Economic Geologists: Littleton, CO, USA, 2005. [[CrossRef](#)]

3. Maier, W.D.; Lahtinen, R.; O'Brien, H. *Mineral Deposits of Finland*; Elsevier: Amsterdam, The Netherlands, 2015; p. 792.
4. Cawthorn, R.G. The Platinum Group Element Deposits of the Bushveld Complex in South Africa. *Platin. Met. Rev.* **2010**, *4*, 205–215. [[CrossRef](#)]
5. Grobler, D.F.; Brits, J.A.N.; Maier, W.D.; Crossingham, A. Litho- and Chemostratigraphy of the Flatreef PGE Deposit, Northern Bushveld Complex. *Miner. Depos.* **2019**, *54*, 3–28. [[CrossRef](#)]
6. Kislov, E.V.; Khudyakova, L.I. Yoko–Dovyren Layered Massif: Composition, Mineralization, Overburden and Dump Rock Utilization. *Minerals* **2020**, *10*, 682. [[CrossRef](#)]
7. Iljina, M. The Portimo Layered Igneous Complex: With Emphasis on Diverse Sulphide and Platinum–Group Element Deposits. Ph.D. Thesis, University of Oulu, Oulu, Finland, 1994; p. 158.
8. Rasilainen, K.; Eilu, P.; Halkoaho, T.; Iljina, M.; Karinen, T. Quantitative Mineral Resource Assessment of Undiscovered PGE Resources in Finland. *Ore Geol. Rev.* **2010**, *38*, 270–287. [[CrossRef](#)]
9. Annen, C. Implications of Incremental Emplacement of Magma Bodies for Magma Differentiation, Thermal Aureole Dimensions and Plutonism–Volcanism Relationships. *Tectonophysics* **2011**, *500*, 3–10. [[CrossRef](#)]
10. Scoates, J.S.; Wall, C.J. Geochronology of Layered Intrusions. In *Layered Intrusions*; Charlier, B., Ed.; Springer: Dordrecht, The Netherlands, 2015; pp. 3–74.
11. Barnes, S.J.; Robertson, J.C. Time Scales and Length Scales in Magma Flow Pathways and the Origin of Magmatic Ni–Cu–PGE Ore Deposits. *Geosci. Front.* **2019**, *10*, 77–87. [[CrossRef](#)]
12. Dortman, N.B. *Physical Properties of Formations and Minerals (Petrophysics): Geophysicist Manual*; Nedra: Moscow, Russian, 1984; p. 455.
13. Karykowski, B.T.; Maier, W.D.; Groshev, N.Y.; Barnes, S.J.; Pripachkin, P.V.; McDonald, I.; Savard, D. Critical Controls on the Formation of Contact-Style PGE–Ni–Cu Mineralization: Evidence from the Paleoproterozoic Monchegorsk Complex, Kola Region, Russia. *Econ. Geol.* **2018**, *113*, 911–935. [[CrossRef](#)]
14. Stepenshchikov, D.G.; Groshev, N.Y. The Application Software for Thermal Modeling of Intrusions. *Tr. FNS* **2019**, *16*, 565–567. [[CrossRef](#)]
15. Mudd, G.M.; Jowitt, S.M.; Werner, T.T. Global Platinum Group Element Resources, Reserves and Mining—A Critical Assessment. *Sci. Total Environ.* **2018**, *622–623*, 614–625. [[CrossRef](#)]
16. Fedorova Tundra, Europe's Largest Deposit of Platinum Group Metals. Available online: <https://fedorovresources.ru/ru/#field> (accessed on 22 March 2022).
17. The Suhanko Project Could Be the Next Mining Operation to Be Implemented in Finland. Available online: <https://www.suhanko.com/what> (accessed on 22 March 2022).
18. Alapieti, T.T.; Filén, B.A.; Lahtinen, J.J.; Lavrov, M.M.; Smolkin, V.F.; Voitsekhovskiy, S.N. Early Proterozoic Layered Intrusions in the Northeastern Part of the Fennoscandian Shield. *Mineral. Petrol.* **1990**, *42*, 1–22. [[CrossRef](#)]
19. Sharkov, E.V.; Chistyakov, A.V. Geological and Petrological Aspects of Ni–Cu–PGE Mineralization in the Early Paleoproterozoic Monchegorsk Layered Mafic–Ultramafic Complex, Kola Peninsula. *Geol. Ore Depos.* **2014**, *56*, 147–168. [[CrossRef](#)]
20. Mokrushin, A.V.; Smol'kin, V.F. Chromite Mineralization in the Sopcheozero Deposit (Monchegorsk Layered Intrusion, Fennoscandian Shield). *Minerals* **2021**, *11*, 772. [[CrossRef](#)]
21. Karykowski, B.T.; Maier, W.D.; Groshev, N.Y.; Barnes, S.J.; Pripachkin, P.V.; McDonald, I. Origin of Reef-Style PGE Mineralization in the Paleoproterozoic Monchegorsk Complex, Kola Region, Russia. *Econ. Geol.* **2018**, *113*, 1333–1358. [[CrossRef](#)]
22. Groshev, N.Y.; Pripachkin, P.V.; Karykowski, B.T.; Malygina, A.V.; Rodionov, N.V.; Belyatsky, B.V. Genesis of a Magnetite Layer in the Gabbro-10 Intrusion, Monchegorsk Complex, Kola Region: U–Pb SHRIMP-II Dating of Metadiorites. *Geol. Ore Depos.* **2018**, *60*, 486–496. [[CrossRef](#)]
23. Kozlov, E.K. *Natural Series of Nickel-Bearing Intrusion Rocks and Their Metallogeny*; Nauka: Leningrad, Russia, 1973; p. 276.
24. Chashchin, V.V.; Bayanova, T.B.; Mitrofanov, F.P.; Serov, P.A. Low-Sulfide PGE Ores in Paleoproterozoic Monchegorsk Pluton and Massifs of Its Southern Framing, Kola Peninsula, Russia: Geological Characteristic and Isotopic Geochronological Evidence of Polychronous Ore–Magmatic Systems. *Geol. Ore Depos.* **2016**, *58*, 37–57. [[CrossRef](#)]
25. Chashchin, V.V.; Mitrofanov, F.P. The Paleoproterozoic Imandra–Varzuga Rifting Structure (Kola Peninsula): Intrusive Magmatism and Minerageny. *Geodin. Tektonofiz.* **2015**, *5*, 231–256. [[CrossRef](#)]
26. Fedotov, Z.A.; Serov, P.A.; Elizarov, D.V. Tholeiites from the Depleted Subcontinental Mantle in the Root Zone of the Monchegorsk Pluton, Baltic Shield. *Dokl. Earth Sci.* **2009**, *429*, 1462–1466. [[CrossRef](#)]
27. Huppert, H.E.; Stephen, R.; Sparks, J. Cooling and Contamination of Mafic and Ultramafic Magmas during Ascent through Continental Crust. *Earth Planet. Sci. Lett.* **1985**, *74*, 371–386. [[CrossRef](#)]
28. Singh, J.; Johannes, W. Dehydration Melting of Tonalites. *Part I. Beginning of Melting. Contrib. Mineral. Petrol.* **1996**, *125*, 16–25. [[CrossRef](#)]
29. Rundkvist, T.V.; Bayanova, T.B.; Sergeev, S.A.; Pripachkin, P.V.; Grebnev, R.A. The Paleoproterozoic Vurechuaivench Layered Pt-Bearing Pluton, Kola Peninsula: New Results of the U–Pb (ID-TIMS, SHRIMP) Dating of Baddeleyite and Zircon. *Dokl. Earth Sci.* **2014**, *454*, 1–6. [[CrossRef](#)]
30. Groshev, N.Y.; Malygina, A.V.; Timofeeva, M.G. Nature of High-Magnesian Xenoliths of the Gabbro-10 Intrusion, Monchegorsk Complex, Kola Region. *Vestn. MSTU* **2018**, *21*, 5–17.

31. Chashchin, V.V.; Ivanchenko, V.V. Sulfide PGE-Cu-Ni and Low-Sulfide Pt-Pd Ores of the Monchegorsk Ore Camp (Western Sector of the Arctic): Geological Characteristics, Mineralogical, Geochemical and Genetic Features. *Geol. Geophys.* **2022**, *63*, 622–650.
32. Mitrofanov, F.P.; Smolkin, V.F. *Layered Intrusions of the Monchegorsk Ore District: Petrology, Mineralization, Isotopy, and Deep Structure*; KNTs RAN: Apatity, Russia, 2004.
33. Amelin, Y.V.; Heaman, L.M.; Semenov, V.S. U-Pb Geochronology of Layered Mafic Intrusions in the Eastern Baltic Shield: Implications for the Timing and Duration of Paleoproterozoic Continental Rifting. *Precambrian Res.* **1995**, *75*, 31–46. [[CrossRef](#)]
34. Groshev, N.Y.; Pripachkin, P.V. Geological Setting and Platinum Potential of the Gabbro-10 Massif, Monchegorsk Complex, Kola Region. *Ores Met.* **2018**, *4*, 4–13. [[CrossRef](#)]
35. Wall, C.J.; Scoates, J.S.; Weis, D.; Friedman, R.M.; Amini, M.; Meurer, W.P. The Stillwater Complex: Integrating Zircon Geochronological and Geochemical Constraints on the Age, Emplacement History and Crystallization of a Large, Open-System Layered Intrusion. *J. Petrol.* **2018**, *59*, 153–190. [[CrossRef](#)]
36. Groshev, N.Y.; Rundkvist, T.V.; Karykowski, B.T.; Maier, W.D.; Korchagin, A.U.; Ivanov, A.N.; Junge, M. Low-Sulfide Platinum-Palladium Deposits of the Paleoproterozoic Fedorova-Pana Layered Complex, Kola Region, Russia. *Minerals* **2019**, *9*, 764. [[CrossRef](#)]
37. Schissel, D.; Tsvetkov, A.A.; Mitrofanov, F.P.; Korchagin, A.U. Basal Platinum-Group Element Mineralization in the Fedorov Pansky Layered Mafic Intrusion, Kola Peninsula, Russia. *Econ. Geol.* **2002**, *97*, 1657–1677. [[CrossRef](#)]
38. Subbotin, V.V.; Korchagin, A.U.; Savchenko, E.E. PGE Mineralization of the Fedorova-Pana Ore Complex: Types of Mineralization, Mineral Composition, Features of Genesis. *Her. Kola Sci. Cent. RAS* **2012**, *1*, 55–66.
39. Latypov, R.M.; Mitrofanov, F.P.; Skiba, V.I.; Alapieti, T.T. The Western Pansky Tundra Layered Intrusion, Kola Peninsula: Differentiation Mechanism and Solidification Sequence. *Petrology* **2001**, *9*, 214–251.
40. Groshev, N.Y.; Nitkina, E.A.; Mitrofanov, F.P. Two-Phase Mechanism of the Formation of Platinum-Metal Basites of the Fedorova Tundra Intrusion on the Kola Peninsula: New Data on Geology and Isotope Geochronology. *Dokl. Earth Sci.* **2009**, *427*, 1012–1016. [[CrossRef](#)]
41. Kalinin, A.A. Precious Metal Mineralization in the East Pansky Layered Massif. In Proceedings of the Fennoscandian School of Ore Genesis in Layered Intrusions; Groshev, N.Y., Ed.; Geological institute KSC RAS: Apatity, Russia, 2021; pp. 20–23. [[CrossRef](#)]
42. Staritsina, G.N. Fedorova Tundra Massif of Basic-Ultrabasic Rocks. In *Issues of Geology and Mineralogy, Kola Peninsula*; Kola Branch AS USSR: Apatity, Russia, 1978; pp. 50–91.
43. Bayanova, T.B. *Age of Reference Geological Complexes of the Kola Region and Duration of Magmatic Processes*; Nauka: St. Petersburg, Russia, 2004; p. 174.
44. Maier, W.D.; Barnes, S.-J. Platinum-Group Elements in Silicate Rocks of the Lower, Critical and Main Zones at Union Section, Western Bushveld Complex. *J. Petrol.* **1999**, *40*, 1647–1671. [[CrossRef](#)]
45. Ariskin, A.A.; Frenkel, M.Y.; Barmina, G.S.; Nielsen, R.L. Comagmat: A Fortran Program to Model Magma Differentiation Processes. *Comput. Geosci.* **1993**, *19*, 1155–1170. [[CrossRef](#)]
46. Bohrson, W.A.; Spera, F.J.; Heinonen, J.S.; Brown, G.A.; Scruggs, M.A.; Adams, J.V.; Takach, M.K.; Zeff, G.; Suikkanen, E. Diagnosing Open-System Magmatic Processes Using the Magma Chamber Simulator (MCS): Part I—Major Elements and Phase Equilibria. *Contrib. Mineral. Petrol.* **2020**, *175*, 104. [[CrossRef](#)]
47. Barnes, S.J.; Malitch, K.N.; Yudovskaya, M.A. Introduction to a Special Issue on the Norilsk-Talnakh Ni-Cu-Platinum Group Element Deposits. *Econ. Geol.* **2020**, *115*, 1157–1172. [[CrossRef](#)]
48. Turovtsev, D.M. *Contact Metamorphism of the Noril'sk Intrusions*; Scientific World: Moscow, Russia, 2002; p. 319.
49. Nikulin, I.I.; Mikhailova, Y.A.; Kalashnikov, A.O.; Groshev, N.Y.; Stepenshchikov, D.G.; Pakhomovskiy, Y.A.; Kadyrov, R.I. *Structural, Textural and Material Properties of Sulfide Copper-Nickel Ores*; Kola Science Centre of the Russian Academy of Sciences: Apatity, Russia, 2022; p. 82.
50. Likhachev, A. *Platinum-Copper-Nickel and Platinum Deposits*; Eslan: Moscow, Russia, 2006. (In Russian)
51. Radko, V.A. *Facies of Intrusive and Effusive Magmatism in the Norilsk Region*; A.P. Karpinsky Russian Geological Research Institute (VSEGEI): St. Petersburg, Russia, 2016; p. 226.
52. Barnes, S.J.; Le Vaillant, M.; Godel, B.; Leshner, C.M. Droplets and Bubbles: Solidification of Sulphide-Rich Vapour-Saturated Orthocumulates in the Norilsk-Talnakh Ni-Cu-PGE Ore-Bearing Intrusions. *J. Petrol.* **2019**, *60*, 269–300. [[CrossRef](#)]
53. Sluzhenikin, S.F.; Yudovskaya, M.A.; Barnes, S.J.; Abramova, V.D.; Le Vaillant, M.; Petrenko, D.B.; Grigor'eva, A.V.; Brovchenko, V.D. Low-Sulfide Platinum Group Element Ores of the Norilsk-Talnakh Camp. *Econ. Geol.* **2020**, *115*, 1267–1303. [[CrossRef](#)]
54. Schoneveld, L.; Barnes, S.J.; Godel, B.; Le Vaillant, M.; Yudovskaya, M.A.; Kamenetsky, V.; Sluzhenikin, S.F. Oxide-Sulfide-Melt-Bubble Interactions in Spinel-Rich Taxitic Rocks of the Norilsk-Talnakh Intrusions, Polar Siberia. *Econ. Geol.* **2020**, *115*, 1305–1320. [[CrossRef](#)]

Disclaimer/Publisher's Note: The statements, opinions and data contained in all publications are solely those of the individual author(s) and contributor(s) and not of MDPI and/or the editor(s). MDPI and/or the editor(s) disclaim responsibility for any injury to people or property resulting from any ideas, methods, instructions or products referred to in the content.